A Novel Model for Drying Refractory Castables

J. Pötschke

Objective of this research is to optimize the time course of the temperature increase during the drying of refractory castables so as to avoid spalling as a consequence of vapour explosion. The heating rate k should be selected so that the temperature curve in the castable is as flat as possible. In the first heating period t the integral mean value of the temperature profile in the refractory castable ϑ_{IMV} should remain < 200 °C, until the cold face of the castable exceeds 110 °C. With this proviso, k can be calculated approximately:

$$\frac{\vartheta_0 - \vartheta_a}{\vartheta_{IMV} - \vartheta_a} = \frac{\sqrt{L}}{3000 \cdot a^{0.25}} \cdot \frac{t}{3{,}7 \cdot 10^{-3} \cdot t - 33{,}5} \qquad (01)$$

The required heating rate is then:

$$k = \frac{\vartheta_0 - \vartheta_a}{t} \quad \text{[K/s]}. \qquad (02)$$

If ϑ_a = 30 °C (temperature at the beginning of drying), ϑ_{IMV} = 150 °C (estimated); L = 0,2 m (thickness of the castable); t = 86 400 s (24 h) (time of first heating); $a = 9 \cdot 10^{-7}$ m²/s (temperature conductivity of the castable), so according to Eq. (01) results ϑ_0 = 210 °C (surface temperature after first heating). It follows from Eq. (02) that the heating rate k = 0,0021 K/s (7,5 K/h) (cf. Fig. 6 black temperature curve). With this value k heating should continue. Empirical values determined in practice should be inserted in Eqs. (01 and 02). They only apply to slow heating and times > 3 h.

1 Introduction

The drying of ceramic materials containing water is a complex process. The drying of tiles, for example, differs considerably from that of refractory castable. The clay brick body contains around 15 mass-% water, an Ultra Low Cement Castable (ULCC) around 5 mass-%. For tiles, there is a danger of shrinkage cracks, while ULCC is prone to explosive spalling if dried improperly.

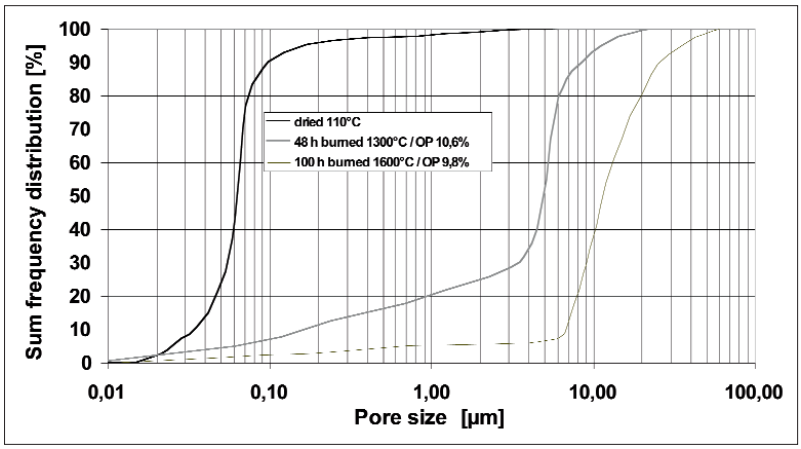

Fig. 1 Pore size distribution of an ULCC

In both cases, a programmed time-temperature curve is preferred. Here bricks are heated slowly to around 110 °C, while refractory material is heated to more than 600 °C.

Jürgen Pötschke
45219 Essen
Germany

E-mail: jpoet@t-online.de

Keywords: drying, spalling, refractory castables, heating rate, temperature conductivity, calculation of drying parameters

Received: 09.10.2009
Accepted: 22.01.2010

Mathematical models facilitate definition of the temperature-time programme. For the clay brick and tile industry, *K. Junge, U. Telljohann* and *A. Tretau* [1, 2] have developed a numerical calculation model. For the drying of refractory castables, *I. Grosswendt* [3] has also come up with such a model.
Objective of this research is to develop a simple and user-friendly analytical model for the drying of refractory castables on the basis of available experience.

2 Basic information

2.1 Refractory castables

Refractory castables consist – in chemical terms – of Al_2O_3, CaO and SiO_2 but can additionally contain ZrO_2 and MgO. The focus of this study is Ultra Low Cement Castable (ULCC) which besides Al_2O_3 contains only small percentages of CaO (as calcium aluminate) and SiO_2 to improve hydraulic bonding. Main components are spinel/corundum or andalusite. The particle size distribution of the matrix is bimodal, approx. 50 mass-% being classified as coarse grain (1 – 100 µm Ø) and 50 mass-% as fine grain (10^{-2} – 1 µm Ø). The coarse grains against wear go up to 6 mm Ø.
The dry mass has a bulk density of around 2700 kg/m³. Adding to this ca. 5 mass-% water, after a mixing time of around 5 min and densification a fresh refractory castable with an apparent density of 2835 kg/m³ is produced.
After this processing, the castable rests ≥ 24 h, during which time hydraulic binder phases are formed. These are mainly gibbsite ($Al(OH)_3$), monocalcium aluminate hydrate ($CaO \cdot Al_2O_3 \cdot 10\ H_2O$) and, at slightly increased temperature, tricalcium aluminate hydrate ($3\ CaO \cdot Al_2O_3 \cdot 6\ H_2O$) [4]. These hydrates clog up especially the fine pore channels, leading to a distinct restraint of moisture transport in the microstructure. Usually the distribution of open pores is determined after drying at 110 °C, as it is assumed that after the long curing time all hydrates have been formed. A typical pore size distribution of an ULCC is shown in Fig. 1. According to this, 90 % of the open pores are < 0,1 µm. The largest open pores measure 3 – 5 µm.
The hydraulic binder phase decomposes, splitting off water, at temperatures above 150 °C. Three phases are observed:

- Adsorbed water evaporates (≥ 110 °C).
- Calcium aluminate hydrates with a low content of hydrate (CAH_{10}, C_2AH_8, C_3AH_6) decompose; the liberated water boils (< 250 °C). There are indications that due to hydrothermal conditions up to 200 °C further hydrates can be formed (*R. Krebs,* priv. memo).
- The remaining hydrates, particularly gibbsite ($Al(OH)_3$), decompose (≤ 400 °C). Minor traces in interstices remain to around 600 °C [5].

Curing should take place at increased temperature (< 100 °C) and therefore as completely as possible so as to avoid the development of stable hydrates at higher temperatures (up to 200 °C). Although they contain less water they decompose at even higher temperatures. That could lead to a vapour explosion (*R. Krebs*, private memo). Around 50 % of the added water is bound as hydrate; the rest is present free in the microstructure and bonds the grains by means of van der Waals forces.

2.2 Mass transport

A differentiation is made between three drying phases.

2.2.1 First drying phase

In the first drying phase, adsorbed water flows under the influence of the capillary force from the inside to the surface and evaporates there into the heat-conducting air. This evaporation takes place only via the free surface of the castable. The mass flow density $\dot{m}$ is [1–3]:

$$\dot{m} = \frac{\beta}{R_D \cdot T} (P_S(T) - P_L) \quad [kg/m^2 \cdot s] \quad (1)$$

β [m/s] is the mass transfer coefficient, R_D = 0,46 kJ/kg·K is the specific gas constant for water vapour, $P_S(T)$ [Pa] is the saturation vapour pressure of the water on the outer surface of the castable and P_L [Pa] is the vapour pressure in the ambient air. The saturation vapour pressure follows from the classical relationship [6]:

$$P_S(T) = 5 \cdot 10^{10} \cdot \exp\left(-\frac{2250}{460 \cdot T}\right) [Pa] \quad (2)$$

At ϑ = 100 °C (T = 373 K), $P_S = 10^5$ Pa results. At temperatures > 250 °C, the values calculated are somewhat too high as the critical point of the water (ϑ = 373 °C, P_S = 217 bar) is approached. (Better approximations, which, however, are not needed here, can be found in [7, 8]).
The mass transfer coefficient depends crucially on the flow velocity u of the drying gas and can be influenced by the flow [9]:

$$\beta = \sqrt{\frac{4\ D \cdot u}{\pi \cdot z}} \quad [m/s]. \quad (3)$$

Here D [m²/s] is the diffusion coefficient of the water vapour in the drying gas and z [m] a characteristic length.
The diffusion coefficient of the water vapour follows from the relationship [10]:

$$D_D(T) = 2{,}3 \cdot 10^{-5} \left(\frac{T}{273}\right)^{1{,}8} \quad [m^2/s] \quad (4)$$

and results for 90 °C (363 K) to $D_D(363) = 3{,}8 \cdot 10^{-5}$ m²/s.
Assuming turbulent gas flow in the drying chamber, $\beta \approx 0{,}01$ m/s and $P_S \approx 0{,}9 \cdot 10^5$ Pa, so that from Eq. (1) the high mass flow density $\dot{m} = 0{,}005$ kg/(m² · s) results. One shall see that in accordance with practical experience, the mass transfer in the flow boundary layer does not determine the drying rate for the refractory castable.
At this point, shrinkage should be briefly mentioned as this can lead to crack formation during the drying of tiles. Approximately it is calculated from the ratio of the apparent densities of the wet body to the dry body ρ_{we} / ρ_{dr}:

$$S_L = \frac{100}{3}\left(\frac{\rho_{we}}{\rho_{dr}} - 1\right)[\%] \quad (5)$$

With ρ_{dr} = 2700 kg/m³ and ρ_{we} = 2835 kg/m³, it follows that the linear shrinkage S_L = 1,7 %. Compared to brick drying (6 %) this value is generally harmless.
During the drying of refractory castables, the first drying stage is usually complete very quickly on account of the rapid increase in temperature to over 100 °C and is therefore of limited importance in field practice. It is ended as soon as the capillary transport of liquid water to the surface is no longer possible over large areas and the drying plane retreats into the interior.
An important part in this is taken by the pores clogged with hydrate, for the capillary pressure is inversely proportional to the pore diameter:

$$P_\sigma = \frac{4\ \sigma_w \cdot \cos\theta}{d} \quad [Pa] \quad (6)$$

Small pores therefore absorb the water out of the large ones and transport it to the surface. This effect is halted as early as more fine pore channels become clogged up.

If the capillary pressure Eq. (6) is inserted into the Hagen-Poiseuille equation [6] for laminar pipe flow, it follows for the mass flow density:

$$\mathring{m} = \frac{\rho_w}{16} \cdot \frac{\sigma_w \cdot \cos\theta \cdot d}{\eta \cdot L \cdot \mu} \quad [\mathrm{kg/m^2 \cdot s}] \quad (7)$$

$\mathring{m}$ decreases with the falling capillary radius d [m] in a linear function. For the mean pore diameter of the refractory castable shown in Fig. 1, $d = 0{,}6$ µm ($0{,}6 \cdot 10^{-6}$ m), based on the surface tension of the water, $\sigma_w = 0{,}07$ N/m, its wetting angle with the capillary wall $\theta = 0°$ (complete wetting), the dynamic viscosity of the water, $\eta = 3 \cdot 10^{-4}$ Pa · s and its density $\rho_w = 1000$ kg/m³ as well as the thickness of the castable layer $L = 0{,}2$ m, it is possible to obtain the value $m = 0{,}0044$ kg/m² · s and for the smallest diameter $d = 0{,}02$ µm the value $\mathring{m} = 0{,}00015$ kg/m² · s. Here $\mu = 10$ is the diffusion resistance coefficient, which corrects the mass transport actually taking place in the microstructure compared to that in free space. The transport is reduced by the factor of 10 [1–3, 10].

2.2.2 Second drying phase

In the second drying phase, the drying plane retreats back into the castable. The free surface is dry. Evaporation takes place inside at the drying plane. During the drying of refractory castables, this state is reached after a short time as the temperature at the surface soon increases to over 100 °C. The vapour is transported in the already dried layer S_{dr} (initially) by diffusion [1, 2]:

$$\mathring{m} = -\frac{D_D}{\mu \cdot S_{dr}} \cdot \frac{P}{R_D \cdot T} \cdot \ln \frac{P - P_{D0}}{P - P_{DK}} \quad [\mathrm{kg/m^2 \cdot s}] \quad (8)$$

D_D is calculated in accordance with Eq. (4); µ = 10; S_{dr} [m] is the thickness of the already dried layer. P [Pa] is the total pressure of the drying gas, e.g. $P = 10^5$ Pa (1 bar). The driving partial pressure gradient is the mean logarithmic difference between the water vapour partial pressure at the drying plane P_{DK} and that at the surface of the castable P_{DO} [1, 2]. If the temperature at the drying plane is e.g. 60 °C (333 K) and at the free surface 90 °C (363 K), Eq. (2) results in the partial pressures $P_{DK} = 0{,}2 \cdot 10^5$ Pa and $P_{DO} = 0{,}67 \cdot 10^5$ Pa. The mean diffusion coefficient for 75 °C (348 K) D_D (348) = $3{,}6 \cdot 10^{-5}$ m²/s. With $S_{dr} = 0{,}05$ m, at 75 °C it follows that $\mathring{m} = 4 \cdot 10^{-5}$ kg/m² · s.

On account of the rising outside temperature, the water in the material > 110 °C starts to boil [11], leading to the flow of vapour in the capillaries. If the Hagen-Poiseuille equation [6] is applied to the flowing water vapour, the following is obtained as the vapour flow density:

$$\ddot{m} = \frac{d^2 \cdot \rho_D}{32 \cdot \eta_D \cdot \mu \cdot S_{dr}} \cdot (P_S - P) \quad [\mathrm{kg/m^2 \cdot s}] \quad (9)$$

With $d = 3 \cdot 10^{-6}$ m, $\rho_D = 0{,}6$ kg/m³, $\eta_D = 1{,}2 \cdot 10^{-5}$ Pa · s, $\mu = 10$, $S_{dr} = 0{,}05$ m at $\vartheta = 150$ °C (423 K) $P_S = 4{,}6 \cdot 10^5$ Pa, it follows that $\mathring{m} = 0{,}01$ kg/m² · s. For two reasons, this result is only an estimate:

- The Hagen-Poiseuille equation applies to a laminar flow. On substantial overheating of the water, however, a turbulent flow is observed, which impairs the mass flow [11].
- Especially in very fine pore channels, the mean free path length of the water molecules is larger than the pore diameter. Here mass transport takes place on the basis of Knudsen diffusion [6], i.e. faster than on the basis of molecular diffusion or convection [3]. Accordingly, this effect, which can be expected for capillary diameters d < 0,1 µm (1 bar), has no influence for the calculation of a possible restraint of the drying of refractory castables, but is in certain cases conductive to mass transport.

Dangerous is the sudden spalling of refractory castable parts of the lining as a consequence of the spontaneous formation of a vapour bubble. Especially dangerous are temperatures above 200 °C [11, 12]. It is observed that the vapour bubbles are formed in the area in which liquid water is still present, which is substantially overheated, that is the area close behind the drying plane.

This is supported by capillary pressure. On account of the complete wetting of the capillary wall by the water ($\theta = 0°$), the meniscus of the water surface in a pore must be calculated as a negative value. With the numbers used for Eq. (7), Eq. (6) would hypothetically result in $P_\sigma = -4{,}6 \cdot 10^5$ Pa. That is equivalent to the fact that compared to the boiling temperature of a large area of water of 100 °C (1 bar), a boiling temperature is now necessary, which corresponds to the overpressure of +4,6 bar, that is $\vartheta = 149$ °C (nucleation inhibition is not taken into account here).

This observation explains the empirically confirmed fact that water can certainly – compared to 100 °C – be overheated by several hundred degrees [11, 12]. The objective is consequently to control the heating rate so that the temperature at the drying plane enables a steady and rapid removal of the vapour so that the liquid water lying behind does not evaporate explosively. The difficulty is that the temperature of the drying plane and its location are not known.

2.2.3 Third drying phase

In the third drying phase the entire liquid water has already been driven out. Remaining moisture in very narrow interstices and hydrates is removed with further increasing temperature. This accounts for less than 5 % of the initial water content [3] and there is usually no longer a danger of spalling as a result of vapour explosion. If, however, further hydrates with a high decomposition temperature have been formed during heating and if these split off a sufficiently large amount of water that evaporates suddenly, vapour explosion can still occur (*R. Krebs*, personal memo).

2.3 Heat transport

It is necessary to supply the following quantity of heat $Q = q_1 + q_2 + q_3$ to the overall system.

- Heating of the water:

$$q_1 = h_o \cdot \rho_w \cdot C_{pw} \cdot \vartheta \quad [\mathrm{kJ/m^3}] \quad (10)$$

- Evaporation of the water:

$$q_2 = h_o \cdot \rho_w \cdot H_w \quad [\mathrm{kJ/m^3}] \quad (11)$$

- Heating of the castable:

$$q_3 = \rho_{FF} \cdot C_{pFF} \cdot \vartheta \quad [\mathrm{kJ/m^3}] \quad (12)$$

h_0 [kg/kg] is the starting water content, therefore, for example 0,05.

This occurs as a result of heat flow

$$\ddot{Q} = \alpha (\vartheta_L - \vartheta_0) = \frac{\lambda_{FF}}{S_{dr}} (\vartheta_0 - \vartheta_K) \quad [\mathrm{W/m^2}] \quad (13)$$

The quotient $\mathring{Q} / Q$ is assigned to the evapo-rating mass flow density of the water content:

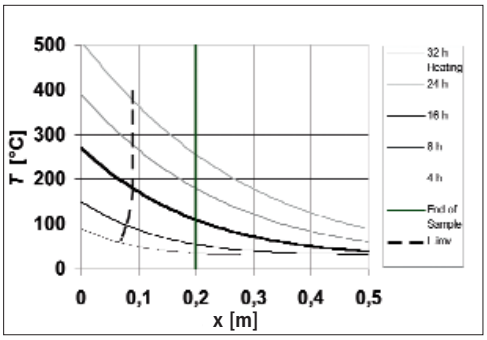

Fig. 2 Curve of the temperature in the castable layer (drying in field practice), (ϑ_a = 30 °C; L = 0,2 m; L_{IMV} = 0,09 m; k = 15 K/h; a = 9 · 10^{-7} m²/s)

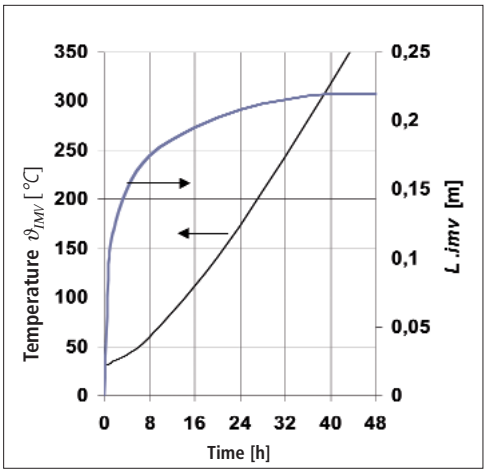

Fig. 3 Course of the integral mean value of the temperature ϑ_{IMV} and the location L_{IMV} as a function of time t (ϑ_a = 30 °C; L = 0,5 m; k = 15 K/h; a = 9 · 10^{-7} m²/s)

$$\dot{m} = \rho_w \cdot \frac{\dot{Q}}{Q} \quad [kg/m^2 \cdot s] \qquad (14)$$

From this, the following results as the drying rate $\dot{m} / p_w$ [13, 14]

$$V_{dr} = \frac{\lambda_{FF}}{S_{dr}\left[(\vartheta_K - \vartheta_a) \cdot (\rho_{FF} \cdot C_{PFF} \cdot \frac{(\vartheta_0 - \vartheta_K)}{+ h_0 \cdot \rho_w \cdot C_{Pw}) + h_0 \cdot \rho_w \cdot \Delta H_w}\right]} [m/s] \qquad (15)$$

ϑ_0 is the temperature at the surface, ϑ_K at the drying plane and ϑ_a at the beginning (see Eq. 32). Experience has shown that the evaporation process is not determined by mass transport [3, 13, 14].

3 Drying model

3.1 Linear heating

In accordance with field practice, control of the temperature determines the drying process of refractory castables. For example, the following heating instruction is given to the customers of an ULCC refractory castable (*H. Dünnes, Calderys*, private memo): after curing and form removal, heating at 15 K/h with a holding time of 1 h / 0,01 m wall thickness at 150 °C, 350 °C and 600 °C. The holding time aids temperature balancing.

Conversely, in laboratory tests, heating rates > 10 K/min are set to provoke spalling and to investigate this [11, 12]. In no case, the location and the temperature of the drying plane are known. They can only be calculated with numerical models [1, 2, 3].

In the following, a simple model for drying refractory castables is developed. It is based on four assumptions:

- Not the mass transport, but the temperature course defines the drying process [3, 13, 14].
- First and second drying stages of refractory castables can be treated the same, as the former is comparatively short [3–5, 11–14] and no explosion occurs.
- As soon as the water has been largely removed, there is no danger for the castable during any further increase of temperature (> 350 °C) [4, 5, 11, 12].
- The integral mean value of the temperature, formed over the total thickness of the castable layer, is a value that approximately replaces knowledge of the exact location of the drying plane and can therefore be used as a basic value for the calculation of the time-temperature curve in the castable. Empirical findings [11, 12] support this assumption insofar that the temperature gradient is steep at this point, so that in the hot, already dried area there is no longer a danger of vapour explosion and this very quickly decreases in the still moist area on account of the cooling. The greatest danger therefore exists just behind the drying front, i.e. close to the integral mean temperature.

For linear heating of an infinitely extended panel, the temperature field follows from (15) as:

$$\frac{\vartheta(x,t,k,a) - \vartheta_a}{\vartheta_0 - \vartheta_a} = \left[\left(1 + \frac{1}{2F_0}\right) \cdot erfc\left(\frac{1}{2\sqrt{F_0}}\right) - \frac{1}{\sqrt{\pi \cdot F_0}} \cdot e^{-\frac{1}{4F_0}}\right] \qquad (16)$$

The surface temperature is

$$\vartheta_0 = \vartheta_a + kt \quad [°C] \qquad (17)$$

with Fourier number

$$F_0 = \frac{a \cdot t}{x^2} \qquad (18)$$

complementary error function

$$erfc\left(\frac{1}{2\sqrt{F_0}}\right) = 1 - \frac{2}{\sqrt{\pi}} \int_0^{\frac{1}{2\sqrt{F_0}}} e^{-y^2}\, dy \qquad (19)$$

x [m] - local coordinate
t [s] - time
a [m²/s] - temperature conductivity of the castable (~ 9 · 10^{-7} m²/s)
k [K/s] - heating rate at the surface
ϑ [°C] - starting temperature of the castable (~ 30 °C).

Fig. 2 shows the temperature curve in the castable layer as an example. The integral mean value of the temperature ϑ_{IMV} at the location L_{IMV} calculated over the entire thickness L of the castable is

$$\vartheta_{IMV} = \frac{1}{L}\int_0^L \vartheta dx = \vartheta a + \frac{k}{6 \cdot L \cdot a^2 \cdot t}\left[erfc\left(\frac{L}{\sqrt{4at}}\right) \cdot (L^3 \cdot a \cdot t + 6L \cdot (a \cdot t)^2) - \pi^{-0,5} \cdot e^{-\frac{L^2}{4at}} \cdot (a \cdot t)^{3/2} \cdot (8a \cdot t + 2L^2) + 8\pi^{-0,5} \cdot (a \cdot t)^{5/2}\right] [°C] \qquad (20)$$

Fig. 3 shows as an example the course of the integral mean value of the temperature and the location over time (T_0 = 30 °C, L = 0,5 m; k = 15 K/h; a = 9 · 10^{-7} m²/s). With the increasing location L_{IMV}, the temperature ϑ_{IMV} rises steadily.

To make the calculation easier, two approximations can be used for Eq. (20).

In short-term tests, therefore in the laboratory, with a run time up to 3 h, the following numerical equation applies:

$$\vartheta_{IMV} \cong \vartheta_a + 2{,}66 \cdot k \cdot t \cdot \sqrt{\frac{a \cdot t}{L}} \quad [°C] \qquad (21)$$

For long-term tests with slow heating, i.e. field practice, the numerical equation applies:

$$\vartheta_{IMV} \cong \vartheta_a + \frac{3 \cdot 10^3 \cdot a^{0,25}}{\sqrt{L}} \cdot$$

$$\cdot k \cdot (3{,}7 \cdot 10^{-3} \cdot t - 33{,}5) \quad [°C] \qquad (22)$$

ϑ_{IMV} describes the integral mean value (*IMV*) of the temperature distribution in the material better, the thicker the layer of castable is as the solutions (Eqs.16 and 20) only apply precisely for an infinitely thick layer of castable. From this, a slice is cut out. This procedure has the practical advantage that thermal conduction in the area behind the wear layer, e.g. in the safety lining, can also be approximately considered.

The given approximations are intended to facilitate a fast estimate. All calculations are, however, done with exact solutions in the scope of this research.

From Eqs. (21) and (22) the heating rate k is obtained that is required to achieve a predefined integral mean value ϑ_{IMV} at the location L_{IMV} in a certain time t. To this end, the values for k and t are chosen so that at the point of the integral mean value L_{IMV}, the temperature is < 200 °C. The temperature gradient in the castable layer should therefore be as flat as possible.

For the rapid heating usual in the laboratory, the following results:

$$k \cong \frac{(\vartheta_{IMV} - \vartheta_a) \cdot \sqrt{L}}{2{,}66 \cdot \sqrt{a} \cdot t^{3/2}} \quad [°C/s] \qquad (23)$$

In field practice, heating takes place very slowly and the following numerical equation applies:

$$k \cong \frac{(\vartheta_{IMV} - \vartheta_a) \cdot}{3 \cdot 10^3 \cdot a^{0,25}}$$

$$\frac{\cdot \sqrt{L}}{(3{,}7 \cdot 10^{-3} \cdot t - 33{,}5)} \quad [°C/s] \qquad (24)$$

If in Eq. (24) k is replaced with Eq. (17), Eq. (01) in the abstract is obtained. Together with Eq. (02), this enables a quick estimate of the heating conditions to avoid vapour explosion.

The location of the mean value temperature L_{IMV} depends on the thickness of the castable layer L and the Fourier number (18):

$$\frac{L_{IMV}}{L} = -6 \cdot 10^{-5} \cdot Fo^6 +$$

$$+ 3 \cdot 10^{-3} \cdot Fo^5 + 4{,}5 \cdot 10^{-2} \, Fo^4 +$$

$$+ 0{,}24 \, Fo^3 - 0{,}62 \, Fo^2 + 0{,}8 \cdot Fo \qquad (25)$$

Fig. 4 shows the curve (black curve) for linear heating, where

$$Fo \equiv Fo_{IMV} = \frac{at}{L_{IMV}^2} \qquad (18a)$$

At each point $P(\vartheta_{IMV}, L_{IMV})$, $\vartheta(x, t, k, a) - \vartheta_{IMV} = 0$ and changes the sign.

For quick estimation of the location L_{IMV} of the integral mean value during heating, Fig. 4 shows that if L_{IMV}/L for $Fo_{IMV} > 2$ it rapidly approaches the limit value 0,45. For $Fo_{IMV} = 2$, $L_{IMV}/L = 0{,}42$ and in most cases it follows from this with acceptable accuracy L_{IMV} 0,45 · L [m]. If $\vartheta_{IMV} < 200$ °C and $\vartheta(L) > 110$ °C, there is hardly any danger of explosion. k and t must be coordinated with each other, for which Eqs. (17 and 21 or 01 and 02, resp.) are used.

3.2 Holding phase

The holding phase has been introduced into practice to achieve slow temperature balancing in the drying refractory castable, i.e. to reduce the danger of vapour explosion. The temperature field is calculated with the same general conditions as before, i.e. for an infinitely extended plate (cf. Eq. (19)):

$$\frac{\vartheta(x,t) - \vartheta_a}{\vartheta_0 - \vartheta_a} = erfc\left(\frac{1}{2\sqrt{Fo}}\right) \qquad (26)$$

Here $\vartheta(t, x)$ is the temperature at the point x at the time t. ϑ_0 [°C] is the temperature of the castable surface ($x = 0$) at the moment of the end of the linear temperature increase, e.g. after 8 h and ϑ_a is the ambient temperature e.g. 30 °C. For the calculation, the temperature field that has developed in the time already lapsed is used.

$$\vartheta_{IMV} = \frac{1}{L}\int_0^L \vartheta dx = \vartheta_a + (\vartheta_0 - \vartheta_a) \cdot$$

$$\cdot \left[erfc\left(\frac{1}{2\sqrt{Fo}}\right) + \frac{2\sqrt{Fo}}{\sqrt{\pi}} \cdot \right.$$

$$\left. \cdot \left(1 - \exp\left(-\frac{1}{4Fo}\right)\right)\right] \quad [°C] \qquad (27)$$

for

$$Fo = \frac{a \cdot t}{L^2} \qquad (18)$$

An approximate solution for Eq. (27) for $Fo < 20$ is:

$$\vartheta_{IMV} \approx \vartheta_a + (\vartheta_0 - \vartheta_a) \cdot$$

$$\cdot \left(-7 \cdot 10^{-3} \, Fo^2 + \right.$$

$$\left. + 0{,}34 \, Fo + 1\right) \quad [°C] \qquad (28)$$

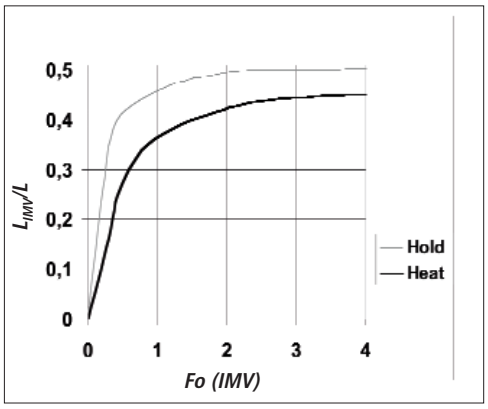

Fig. 4 Curve of the L_{IMV}/L ratio as a function of the Fourier number Fo_{IMV}

for

$$Fo = \frac{a \cdot t}{L^2} \qquad (18)$$

The relationship of the location at which the integral mean value of the temperature is present L_{IMV} to the thickness of the castable layer L as a function of the Fourier number at the point L_{IMV} is given approximately by the polynomial

$$\frac{L_{IMV}}{L} = -0{,}0039 \, Fo^6 + 0{,}0615 Fo^5 -$$

$$- 0{,}3824 \, Fo^4 + 1{,}1817 \, Fo^3 -$$

$$- 1{,}9003 \, Fo^2 + 1{,}5188 \, Fo \qquad (29)$$

This is shown in Fig. 4 (grey curve). It is

$$Fo \equiv Fo_{IMV} = \frac{a \cdot t}{L_{IMV}^2} \qquad (18a)$$

and for $Fo_{IMV} > 1{,}5$ reaches its limit value 0,5. Within the context of the accuracy of the calculations, $(L_{IMV}/L)_{Heat} \sim (L_{IMV}/L)_{Hold}$. The difference is practically negligible.

4 Spalling

Spalling occurs when the liquid water still present beyond the drying plane suddenly evaporates as a result of boiling retardation and the pressure generated tears the material. The vapour bubbles nucleate homogeneously as the wetting angle $\theta = 0$. But the vapour pressure necessary for the formation of an imaginary spherical bubble nucleus can be indicated as the nucleation energy is 1/3 of the surface energy. This tear resistance of the water is [16, 17]:

$$\Delta P = \frac{8\,\sigma}{3\,d} \quad [Pa] \qquad (30)$$

For the largest pore diameter measuring 3 µm (3 · 10^{-6} m), it follows with the surface

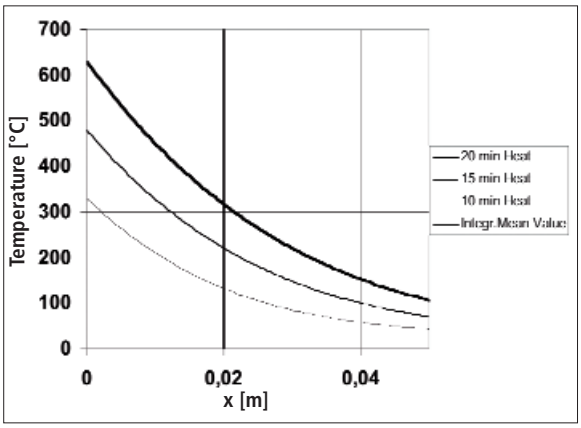

Fig. 5 Preheating and holding temperatures during laboratory drying (ϑ_0 = 30 °C; L = 0,05 m; L_{IMV} = 0,02 m; k = 30 K/min; $a = 9 \cdot 10^{-7}$ m²/s)

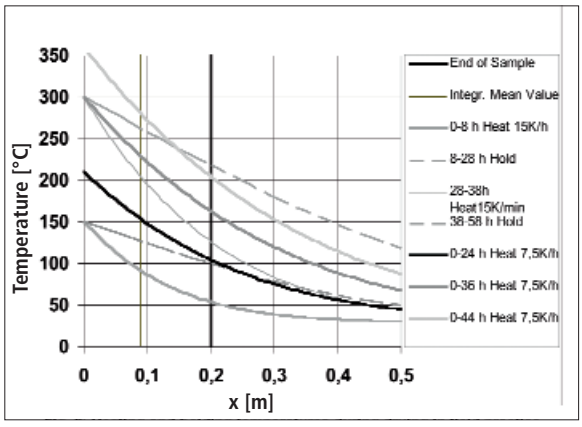

Fig. 6 Heating and holding temperatures during drying in field practice (ϑ_0 = 30 °C; L = 0,2 m; L_{IMV} = 0,09 m; k = 15 K/h; $a = 9 \cdot 10^{-7}$ m²/s)

tension of the water $\sigma \cong 0{,}06$ N/m at 100 °C) $P = 5 \cdot 10^4$ Pa (+0,5 bar). That would be the minimum overpressure at which vapour bubbles are formed. For $d = 0{,}3 \cdot 10^{-6}$ m, $P = 5$ bar already follows as the overpressure. In practice, pressure and temperature will be much higher as the nucleation rate increases exponentially with decreasing bubble radius [16].

The pore structure of the refractory material, however, also has the effect of a "boiling chip", in that during its heat expansion any foreign gas present is pressed into the water and therefore acts as bubble nucleus.

This becomes problematic when water from a hot area is pressed by the high vapour pressure prevailing there into the cold areas of the refractory material. There the effect of the "boiling chip" is namely much less evident as the saturation vapour pressure of the water is higher than the ambient pressure. The result can be spontaneous vapour development, the pressure of which tears the castable. This is comparable to the process in a microwave. In a cooking pot, on the other hand, bubbles are formed at the hot base with only limited boiling retardation at around 110 °C. As vapour explosion is a stochastic process, a lower limit value for the pressure must be determined which must be exceeded for to be a risk of danger [5]. Suitable for this is the tensile strength σ_s of the castable in the cured state, e.g. at 110 °C. In the literature, a wide range of specifications are found between 1,4 MPa [5] and 10 MPa [12], the tensile strength being calculated as around 1/10 of the compressive strength ($\sigma_s \sim 1/10\ \sigma_d$) [18]. According to Eq. (2), 1,5 MPa as the saturation vapour pressure corresponds to a temperature of almost 200 °C and 10 MPa to around 300 °C. That is the temperature range in which spalling occurs. Critical is the temperature range between 200 and 300 °C [12, 13]. The objective is therefore to pass through this temperature range so slowly that any water vapour can be transported outwards without any problem. When reaching 200 °C as the integral mean value, the cold end of the castable should be above 110 °C. The heating rate k should be chosen accordingly.

5 Two examples

5.1 Laboratory tests

H. Abe [11, 12] conducted laboratory tests on vapour explosion during the drying of refractory castables. Summarized, his findings are as follows: Spalling occurs at surface temperatures > 400 °C after 10 – 20 min around 14 – 27 mm below the castable surface. The mean heating rate is 30 K/min and the temperature at the centre of the test specimens (100 mm Ø) is more than 150 °C. The following figures result: L = 0,05 m; $a = 9 \cdot 10^{-7}$ m²/s; k = 30 K/min (1800 K/s); ϑ_a = 30 °C; t = 15 – 20 min (900 – 1200 s); $L_{IMV} \sim$ 0,02 m. The result of the calculation according to Eqs. (16 – 20) is shown in Fig. 5. It can be seen that in the range of the integral mean value $L_{IMV} \sim$ 0,02 m, the temperature lies between 130 °C and 310 °C. That is precisely the empirically observed temperature range. The associated saturation vapour pressure is 3 – 114 bar and on average (20 bar) lies above the pressure previously estimated at around 5 bar. The "cold end" of the specimen only reaches just under 100 °C. For an approximate calculation Eq. (21) has to be used.

5.2 Drying in field practice

As remarked in the introduction, one proposal for the drying of cured castables is as follows:

- Heating at 15 K/h to 150 °C
- Holding over 1 h/0,01 m wall thickness
- Heating at 15 K/h to 350 °C
- Holding over 1 h/0,01 m wall thickness
- Heating to ≥ 600 °C.

This approach avoids vapour explosion. Fig. 6 shows the calculated temperature curves for a castable layer of the thickness L = 0,2 m. For this castable layer, the integral mean value lies at $L_{IMV} = 0{,}45 \cdot 0{,}2 =$ 0,09 m (cf. Fig. 4). In the first heating and holding stage, that is 28 h, the temperature remains subcritical (grey and dashed curves). In the second heating stage, in the area of the integral mean value just 200 °C and at the cold castable end 130 °C are reached (thin grey curve). The critical temperature range from 200 to 270 °C is passed through slowly in the twenty-hour holding phase (dashed curve). From this point in time, in field practice, the material is heated without vapour explosion to much higher than 300 °C. Overall, by the time 300 °C is reached, 58 h have elapsed.

Using Eqs. (01) and (02) three steps are necessary to calculate a continuous heating rate which avoids explosion as well but in a shorter time.

Symbols, definitions and abbreviations

		Equation
a [m²/s]	temperature conductivity of castable	18, 19
C_{PFF} [kJ/kg · K]	specific heat of castable	12
C_{Pw} [kJ/kg · K]	specific heat of water	11
d [m]	capillary radius	6
D [m²/s]	diffusion coefficient	3
D_D (T) [m²/s]	diffusion coefficient of water vapour	4
erfc(Y)	complementary error function	19
Fo	Fourier number	18
Fo_{IMV}	Fourier number at integral mean number	18a
h_0 [kg/kg]	starting water content	11
ΔH_w [kJ/kg]	heat of water evaporation	11
k [K/s]	heating rate at surface of castable	17, 19
L [m]	thickness of castable layer	7
L_{IMV}[m]	thickness of castable layer at integral mean value	18a
$\mathring{m}$ [kg/m² · s]	mass flow density	1
$\mathring{m}_P$ [kg/m² · s]	mass flow density dependant on pressure difference	31
m_ϑ [kg/m²·s]	mass flow density dependant on temperature difference	32
P [Pa]	total pressure of drying gas	8
ΔP [Pa]	pressure difference	30
P_{DK} [Pa]	vapour partial pressure at drying plane	8
P_{DO} [Pa]	vapour partial pressure at surface of castable	8
P_L [Pa]	vapour pressure in ambient air	1
P_S (T) [Pa]	saturation vapour pressure of water	2
P_σ [Pa]	capillary pressure	6
$\mathring{Q}$, q_1, q_2, q_3 [kJ/m³]	quantity of heat	10–13
$\mathring{Q}$ [W/m²]	heat flow	13
R_D [kJ/kg·K]	specific gas constant for water vapour	1
S_{dr} [m]	thickness of already dried layer	8
S_L [%]	linear shrinkage	5
t [s]	time	18, 19
T [K]	temperature	1
u [m/s]	flow velocity of drying gas	3
V_{dr} [m/s]	drying rate	15
x [m]	local coordinate	18, 19
z [m]	characteristic length	3
α [W/m²·K]	heat flow coefficient	13
ß [m/s]	mass transfer coefficient	3
η [Pa·s]	dynamic viscosity of water	7
η_D [Pa·s]	dynamic viscosity of water	9
λ_{FF} [kW/m·K]	thermal cemperature conductivity of refractory castable	13
μ [-]	diffusion resistance coefficient	7
ρ_{dr} [kg/m³]	apparent density of dry body	5
ρ_{we} [kg/m³]	apparent density of wet body	5
ρ_w [kg/m³]	density of water	10
ρ_{FF} [kg/m³]	bulk density of refractory material	12
σ_w [N/m]	surface tension of water	
ϑ [°C]	temperature	2
$\Delta\vartheta$ [°C]	temperature difference	10
ϑ_K [°C]	temperature at drying plane	13
ϑ_α [°C]	surface temperature of castable at beginning	15, 16
ϑ_0 [°C]	surface temperature of castable after heating	13, 16
ϑ_{IMC} [°C]	temperature of integral mean value	20
θ [°]	wetting angle	6

- Step 1:
  Assume a surface temperature of e.g. ϑ_0 = 210 °C and the starting temperature ϑ_a = 30 °C, the thickness of the castable layer L = 0,2 m and its temperature conductivity $a = 9 \cdot 10^{-7}$ m²/s. After a time of 24 h (86 400 s) the integral mean value of the temperature results in ϑ_{IMV} = 150 °C.
- Step 2:
  Take the thickness of the castable layer L = 0,2 m as the location of the (new) integral mean temperature ϑ_{IMV} of a fictive castable of the thickness L = 0,2 m / 0,425 = 0,5 m (see Fig. 4). Calculate its temperature by using Eq. (01) and the above values ϑ_0 = 210 °C, ϑ_a = 30 °C, a = $9 \cdot 10^{-7}$ m²/s, t = 24 h and L = 0,5 m which results in ϑ_{IMV} = 110 °C. That is the temperature of the backside of the castable layer.
- Step 3:
  From Eq. (02) we get as the heating rate k = 7,5 K/h.

These values should be subcritical in respect to explosion because they are similar to the a.m. practical findings. The same applies for the surface temperatures 300 °C and 360 °C (Fig. 6). In addition it should be mentioned that in praxis 58 h are used and by continuous heating only 44 h.

6 Rates of vapour eduction

As the temperature range of the vapour explosion is very wide at 200 – 300 °C, for this case it should be estimated how the rates of vapour eduction and the temperature increase behave in relation to one another. For this purpose Eqs. (9) and (15) are used as:

$$\mathring{m}_P = \frac{d^2 \cdot \rho_D}{32 \cdot \eta_D \cdot \mu \cdot L_{IMV}} \cdot \cdot \left(P_S - P\right) \quad [\text{kg/m}^2\cdot\text{s}] \qquad (31)$$

and

$$\frac{\lambda_{FF} \cdot (\vartheta_0 - \vartheta_{IMV}) \cdot \rho_W}{\left[(\vartheta_{IMV} - \vartheta_a) \cdot (\rho_{FF} \cdot C_{PFF} + h_0 \cdot \rho_w \cdot C_{Pw}) \cdot \frac{1}{+ h_0 \cdot \rho_w \cdot \Delta H_w}\right] \cdot L_{IMV}} \quad [\text{kg/m}^2\cdot\text{s}] \qquad (32)$$

With the physical characteristics

- Thermal conductivity of the refractory castable $\lambda_{FF} = 2{,}5 \cdot 10^{-3}$ kW/m · K

• Surface temperature of the castable
ϑ_0 = 210 °C
• Temperature of the integral mean value:
ϑ_{IMC} = 150 °C
• Already dried distance
L_{IMV} = 0,09 m (of 0,2 m)
• Density of the refractory castable
ρ_{FF} = 2700 kg/m³
• Specific heat of the castable
C_{PFF} = 1 kJ/kg · K
• Mixing water content
h_0 = 4,5 kg/100 kg castable = 0,045
• Density of the water
ρ_W = 917 kg/m³
• Specific heat of the water
C_{Pw} = 4,3 kJ/kg · K
• Heat of water evaporation
H_w = 2257 kJ/kg
• Mean heating of the water and the refractory castable $\vartheta_{IMV} - \vartheta_a$ = 120 °C
• Density of the water vapour
ρ_D = 2,5 kg/m³
• Mean temperature difference between the surface and the drying plane:
$\vartheta_0 - \vartheta_{IMV}$ = 60 °C
• Pore diameter $d = 3 \cdot 10^{-6}$ m
• Viscosity of the vapour
$\eta_D = 1{,}4 \cdot 10^{-5}$ Pa · s
• Diffusion resistance coefficient μ = 10
• Vapour pressure $P_S = > 5 \cdot 10^5$ Pa
• Air pressure P = 10^5 Pa
it follows:

$$\dot{m}_P = 5 \cdot 10^{-9} \cdot \left(P_S - 10^5\right) / L_{IMW} \text{ [kg/m}^2\text{·s]}$$

i. e. $\dot{m}_D > 20 \cdot 10^{-4} / L_{IMW}$ [kg/m²·s].
Crucial is the temperature range > 150 °C, i.e. $P_s \geq 5 \cdot 10^5$ Pa.
On the basis of the heat supply, the drying rate is calculated as follows:

$$\dot{m}_{th} = 3 \cdot 10^{-4} / L_{IMV} \text{ [kg/m}^2\text{·s]}$$

As already mentioned several times, mass transport is faster than the heat transport, i.e. there is no build-up of vapour and the danger of explosion is low. With increasing temperature, this effect increases as the vapour pressure grows exponentially.

Acknowledgement

I wish to thank *Dr M. Hopf*, Ilmenau, for giving the idea for this research, *Dipl.-Ing. E. Brochen*, Bonn, for his assistance with some numerical calculations and *Dipl.-Ing. C. Brüggmann*, Bonn, for his useful comments. I thank Messrs *Dipl.-Ing. H. Dünnes,* Neuwied, *Dipl.-Ing. R. Krebs*, St. Augustin, and *Dipl.-Ing. G. Routschka*, St. Augustin, for providing data and information from field practice and literature. *Dr K. Junge*, Essen, and *Dr A. Tretau*, Essen, gave me a lot of help discussing about drying of tiles for what I am very grateful. I am grateful as well to *Dr P. Röhl*, Essen, who corrected the manuscript. My thanks also go to *Prof. Dr P. Quirmbach*, Bonn, and the Ministry for Research and Technology, represented by the AIF, by the project number AIF 6 EN, for their support.

References

[1] Junge, K.; Telljohann, U.: Trocknung von Ziegelrohlingen – Einfluss der Feuchteleitfähigkeit auf Schwindungsfortschritt und Trocknungsverlauf. ZI-Jahrbuch (2005) 21 ff.
[2] Junge, K.; Tretau, A.: Energieaufwand zur Rohlingstrocknung in Kammertrocknern. ZI-Jahrbuch (2007) 25 ff.
[3] Großwendt, I.: Modell zur Beschreibung der Trocknung von Feuerbetonen. Dr.-Ing. Diss. 2007, RWTH Aachen
[4] Akiyoshi, M.M.; Cardoso, F.A.; Innocenti, M.D.M.; Pandolfelli, V.C.: Key properties for the optimization of refractory castable drying. Refr.Applications and News 9 (2004) [4] 14–16
[5] Innocenti, M.D.M.; Miranda, M.F.S.; Cardoso, F.A.; Pandolfelli, V.C.: Vaporization process and pressure bild-up during dewatering of dense refractory castable. J. Am. Ceram. Soc. 86 (2003) 1500–1503
[6] Gerthsen, C.; Meschede, D.: Physik. Springer, 2005
[7] Reid, R.G.; Prausnitz, J.M.; Poling, B.E.: The properties of gases and liquids. Mc Graw-Hill, (1989) 208–209
[8] Junge, K.: Daten zur feuchten Luft-Trockungstechnik. ZI-Jahrbuch (1996) 128–137
[9] Bird, R.B.; Stewart, W.E.; Lightfoot, E.N.: Transport phenomena. J. Whiley Sons, N.Y. (1960) 541
[10] Grunewald, J.: Vorl. "Bauphysik", TU Dresden, 2009
[11] Abe, H.: Drying mechanism of castable refractories. J. Techn. Ass. Refractories, Japan 23 (2003) [3] 164–170
[12] Abe, H.: The effect of permeability on the explosion of castables during drying. J. Techn. Ass. Refractories, Japan 24 (2004) [2] 115–119
[13] Block, F.R.; Geber, H.; Gross, C.; Pernot, J.; Zografou, C.: Temperatur und Trocknungsüberwachung bei der Herstellung monolithischer Bauteile. Proc. 37. Int. Colloquium on Refractories, Aachen, 1994, pp. 210–217
[14] Schmitz, W.; Bank, H.; Block, F.R.; Geber, H.; Groß, C.; Manga, D.; Maier, H.R.; Franken, K.; Metzlaff, K.: Messtechnische Überwachung des Aufheizens und Trocknens der feuerfesten Zustellung. Proc. 38. Int. Colloquium on Refractories, Aachen, 1995, 48–56
[15] Carlslaw, H.S.; Jaeger, J.C.: Conduction of heat in solids. Oxford Univ Press, 2. Ed., 1959
[16] Volmer, M.: Kinetik der Phasenbildung. Steinkopf, Dresden, 1939, S. 161
[17] Pötschke, J.: Entstehung und Verhalten von Ausscheidungen bei der Erstarrung. In: Erstarrung metallischer Schmelzen. DGM 1981, S. 221–231
[18] Routschka, G.: Refractory Materials, 2. Ed., Vulkan Verlag, Essen